FINITE ELEMENT MODELING OF SMALL-SCALE TAPERED WOOD-LAMINATED COMPOSITE POLES WITH BIOMIMICRY FEATURES[1]

Cheng Piao†

Assistant Professor
Calhoun Research Station
Louisiana State University AgCenter
Calhoun, LA 71225

Todd F. Shupe†

Professor
Louisiana Forest Products Development Center
School of Renewable Natural Resources
Louisiana State University AgCenter
Baton Rouge, LA 70803

R. C. Tang†

Professor
School of Forestry & Wildlife Sciences
Auburn University
Auburn, AL 36849

and

Chung Y. Hse

Principal Wood Scientist
USDA Forest Service
Southern Research Station
2500 Shreveport
Pineville, LA 71360

(Received November 2006)

ABSTRACT

Tapered composite poles with biomimicry features as in bamboo are a new generation of wood laminated composite poles that may some day be considered as an alternative to solid wood poles that are widely used in the transmission and telecommunication fields. Five finite element models were developed with ANSYS to predict and assess the performance of five types of composites members: a tapered hollow pole with webs (Pole-A), a tapered hollow pole without webs (Pole-B), a tapered solid composite pole (Pole-C), a uniform-diameter hollow pole with webs (Pole-D), and a uniform-diameter hollow pole without webs (Pole-E). The predicted deflection by these models agreed well with those of the experiment, and the predicted normal stress agreed with those calculated. The normal and shear stress distributions inside the members were investigated, and stress distributions in the XY and YZ planes are exhibited. As expected, the webs reduced the local shear stress and improved shear capacity, especially in the top and groundline regions where shear levels were the highest. The webs had little effect on the normal stress. Shear stress increased from the bottom to the top for the members with taper. Large shear stress con-

---

centration was predicted in a small region close to the groundlines. The models also predicted that the shear stress of the tapered hollow poles would decrease from the inside to the outside surfaces in XY plane.

Keywords: Biomimicking, composite poles, finite element analysis, shear stress, taper.

INTRODUCTION

Wood is a traditional material for utility poles that are widely used in power transmission and telecommunication fields around the world. Every year millions of new wood poles are installed to carry overhead cables for electricity and telephone in the United States. When compared with other materials used in these utility fields such as concrete, steel, and fiberglass, wood poles are light, easy to climb, strong, and easily machined. Wood poles are produced from a renewable natural resource, which is resilient and environment-friendly if properly preservative-treated. Although post-construction costs, such as inspection, maintenance, repair, replacement, and disposal are higher, wood poles remain the cost-effective choice (AWPI 1996).

In the last few decades, high quality tree-length logs suitable for transmission and distribution poles have been in great demand. Millions of new poles are required in either construction of new lines (Bratkovich 2002) or replacement of poles that failed in service because of decay, termite attack, and hurricane/storm. Moreover, poles may become obsolete or suffer mechanical damage and be taken out of service. Many approaches have been investigated as an alternative to solid poles to more efficiently utilize wood. These alternatives that are published in the literature include glulam poles (Hockaday 1975; McKain 1975), mechanical-fastened wood composite poles (Marzouk et al. 1978), pressed wood flake poles (Adams et al. 1981), reinforced plastics jacketed (RPJ) composite poles (Tang and Adams 1973), hollow veneered poles (HVP) (Erickson 1994 and 1995). Most recently, hollow wood laminated composite poles with a uniform diameter through the pole length were developed (Piao et al. 2004). Experimental tests of the poles in cantilever bending showed that shear failure in the neutral plane was a major failure mode. The clamped length at test, shell thickness, adhesion defects, early wood, and wood grain directions were among the major factors that affected the failure mode and the loading capacity of the composite poles. To improve the shear capacity and member integrity, node-like webs (hereinafter referred to as webs) and taper that were biomimicked from bamboo structure were introduced into the design of a new generation of hollow composite poles (Piao et al. 2006). Results showed that plywood webs reduced the propagation of spring-wood failure along pole length. The tapered poles tested had longer failure zones but exhibited higher modulus of rupture (MOR) per weight and modulus of elasticity (MOE) per weight than those of poles with uniform diameter through pole length.

A finite element model has been developed to predict the performance of the uniform-diameter composite poles subjected to loads (Piao et al. 2005). Results showed that the predicted deflection for both small-scaled and full-size composite poles agreed well with those measured in the experiment. To assess the stress distribution characteristics and optimize the design of node-like webs and taper angles, it is necessary to develop finite element models for the poles coupled with biomimicry concepts. Biomimicry is a new science that studies nature's models and then imitates or takes inspiration from these designs and processes to solve human problems (Biomimicry 2006). The objective of this study was to compare the results of finite element modeling of five small-scaled wood laminated composite poles subjected to the same loading conditions as those of the poles tested in our previous experimental study (Piao et al. 2006). The design optimization of the composite poles using finite element modeling will be conducted in the next study.

EXPERIMENTAL STUDY

Five finite element models were developed in this study to simulate the five corresponding composite poles in the previous study (Piao et al. 2006) to gain a complete understanding of the behavioral characteristics of these newly designed structural members under load. These poles include a round tapered hollow pole with plywood webs (Pole-A), a round tapered hollow pole without webs (Pole-B), a round tapered solid composite pole (Pole-C), a uniform-diameter polygonal hollow pole with plywood webs (Pole-D), and a uniform-diameter polygonal hollow pole without webs (Pole-E). All three tapered poles had a taper of approximately 0.3 degree. Each of the hollow and nodal poles was made from nine pieces of trapezoid southern pine (*Pinus* spp.) wood strips bonded with a resorcinol formaldehyde (RPF) resin. All fabricated poles were 2.4 m in length and 102 mm in circumscribed diameter (typical full-size poles could be from 6.1 m to 21.3 m in length and from 250 mm to 410 mm in diameter at 1.8 m from the butt). The reasons for selecting small-scaled sizes of poles as the experimental materials were (1) the manufacturing process of small-scale composite poles was very similar to that of a full-scale composite pole, and (2) the major objective of this research was to test the effects of taper and node-like plywood webs on the performance of the hollow wood composite poles. Strip thickness was 30 mm. The length of plywood webs was 57.2 mm and diameter was 18.9 mm. The webs were first wrapped with four layers of Kraft paper that was impregnated with RPF resin. Then they were placed inside the pole at an interval of every 610 mm along the pole length axis and in both ends of each member. These webs were simulated from the natural structure of bamboo to (1) reinforce the pole in shear capacity, and (2) regulate the moisture effects from above and under the ground on the poles. At the clamped line (groundline), three such webs were placed to improve the stress distribution of the pole in the cantilever bending test. All poles were modeled in cantilever bending. The models developed may pave the way

for the design and analysis of using biomimicry for wood laminated composite poles with similar structural characteristics to the ones presented in this paper.

Analytical procedures

The analytical procedure involved parametrically modeling the deflection and normal and shear stress of five composite poles with biomimicry features with ANSYS, a commercial finite element modeling software developed by ANSYS, Inc. In the modeling, both hollow and solid composite poles were analyzed as orthotropic materials. Each hollow composite pole was viewed as a glued volume composition of trapezoid wood strips, rectangular prism gluelines and/or polygonal webs. A tetrahedral element type with 10 nodes each having three degrees of freedom was assigned to each member. This element type has a nonlinear displacement behavior, plasticity, large deflection, and large strain capabilities. Figure 1 shows the element and its nodes.

In ANSYS, the graphical representation of the tapered hollow poles (Pole-A and Pole-B) was formed by sweeping a quadrilateral about the *z* axis (longitudinal direction). The quadrilateral was composed of two radii of the top and bottom cross-sections of the pole to be formed, an axial line connected the two radii, and another straight
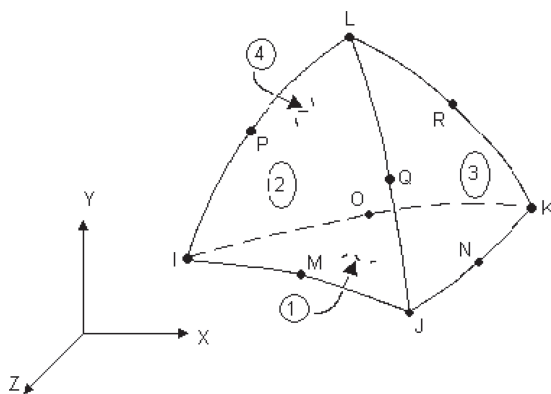

FIG. 1. Three-dimensional 10-node tetrahedral structural solid used in the finite element modeling of wood laminated composite poles with bio-mimicking features.

line connected the other end of the two radii. After several subtraction and extrusion (Boolean) operations on the tapered solid body, a composite pole consisting of 9 strips, 9 gluelines, and/or 4 webs was formed. Similar procedures were used in forming the tapered solid pole (Pole-C). For the two uniform-diameter poles, Pole-D and Pole-E, cross areas of the gluelines and strips were created and extruded along the z axis. In the final step, all members were glued to create a pole model for each of the five members.

These three kinds of volumes were meshed separately due to the difference in the element sizes. Gluelines in both solid and hollow poles were treated as thin volumes. Each glueline had uniform thickness, which was assumed 0.2 mm for both hollow and solid composite poles. The width-to-depth ratio of the gluelines was 160 for hollow and nodal poles and 506 for the solid pole in the bottom cross-sections. To elementize or mesh such thin volumes, small element sizes were necessary to obtain desirable and computable element models for wood strips, gluelines, and webs. Line division, an operation of ANSYS, was applied to the radial lines of each glueline at top and bottom cross-sections of each pole to further reduce the element sizes. Relatively larger element sizes were selected in the meshing of wood strips and webs to reduce the number of elements and computation time. However, where gluelines separate wood strips and webs, an increase in the element sizes of wood strips and webs would not greatly reduce the total number of the elements when the glueline element size was set.

The Young's moduli of the poles in the z direction were the modulus of elasticity (MOE) values obtained from the previous experimental study (Piao et al. 2006). The plywood webs and RPF-impregnated Kraft papers wrapped outside the webs were treated as one material in the modeling. The constitutive properties of these webs were approximated by the constitutive properties of the plywood used. Other constitutive properties of wood and all constitutive properties of nodal materials (plywood) were obtained from the Wood Handbook (USDA FPL 1999). Constitutive properties of RPF resin were obtained from the Adhesive Handbook (Shidles 1970). Table 1 lists the constitutive properties of wood, plywood, and gluelines. Wood strips and plywood webs were assumed to be orthotropic materials, while gluelines were assumed an isotropic material. It is well known that the interface between wood and RPF is a complex matrix and was simplified in this study as two clean volumes that were glued together.

Table 2 lists the shape specifications of the poles, gluelines, and node-like webs used in this modeling. The deflection and stress of each pole under a concentrated load at its free end were modeled. The size parameters of each pole were held constant and equated to parameters corresponding to the pole that the model simulated. Each pole was simulated at five consecutive loading levels (222, 311, 400, 533, and 667 N). The deflections and normal stresses along each pole were determined by retrieving the deflection and stress values of the nodes on the top surface of the pole. The shear stress under each load was determined by the shear stress of the

TABLE 1. *Constitutive properties of wood[1], resorcinol phenol-formaldehyde (RPF) resin[2], and plywood[3].*

Pole types	E_x (10^3 MPa)	E_y (10^3 MPa)	E_z (10^3 MPa)	G_{xy} (MPa)	G_{yz} (MPa)	G_{xz} (MPa)	v_{xy}	v_{yz}	v_{xz}
A	1.2	1.2	11.5	149.7	938.3	938.3	0.38	0.30	0.30
B	1.2	1.2	11.4	149.7	938.3	938.3	0.38	0.30	0.30
C	1.2	1.2	12.6	149.7	938.3	938.3	0.38	0.30	0.30
D	1.2	1.2	10.1	149.7	938.3	938.3	0.38	0.30	0.30
E	1.2	1.2	8.1	149.7	938.3	938.3	0.38	0.30	0.30
RPF	4.5	4.5	4.5	500.0	500.0	500.0	0.20	0.20	0.20
Plywood	12.5	10.8	1.3	938.3	150.0	150.0	0.15	0.14	0.14

[1] Southern yellow pine (*Pinus* sp.). Wood Handbook (USDA FPL 1999).
[2] Adhesive Handbook (Shidles 1970).
[3] Wood Handbook (USDA FPL 1999).

TABLE 2. *Specifications of wood laminated composite poles in the finite element modeling.*

Pole length (mm)	Pole diameter (mm)	Strip thickness (mm)	Glueline thickness (mm)	Web length (mm)	Taper angle (degree)
1828.8	101.6	30.0	0.2	57.2	0.3

nodes on one side of the pole surface in the neutral plane. These shear values may not be the maximum under a specific load level but will display the shear variation along the pole. Deflections and normal stresses were compared to the corresponding deflections and stresses obtained from the experiment.

The bending and shear stresses along the tapered and uniform poles were calculated for comparison to those results from the finite element modeling. The effect of pole weight on deflection and stress was neglected for all the models. The effect of shear on deflection was also neglected in the calculation. The normal stress along the tapered pole was calculated by using the following formula:

$$\sigma = \frac{4Pl}{\pi R^3} \left(\frac{R^4}{R^4 - r^4} \right) \qquad (1)$$

where P is the loading force, l is the distance from tip to the interested cross-section, R is the radius of the interested cross-section, and r is the radius of the hollow part of the cross-section. Because the part in parentheses in Eq. (1) is relatively small, the normal stresses of the poles were calculated as solid poles. Shear stress of both tapered and uniform poles was evaluated by using the following formula (Gere and Timoshenko 1990):

$$\tau = \frac{VQ}{It} \qquad (2)$$

where V is the shear force, Q is the first moment of the interested cross-section, I is the moment of inertia of the cross-section, and t is the sum of pole shell thickness at the measured section.

RESULTS AND DISCUSSION

In formulating (Boolean operations) and/or meshing the gluelines with ANSYS, program failures occurred when some physical dimensions and glueline element sizes were used. This shows the limitation of ANSYS in modeling members with difficult geometries. When such a case occurred, alternative line divisions or element sizes were used. The modeling was conducted in a desktop computer with a Pentium® III processor. The total number of equations was from 110,000 to 200,000 for the 5 models. The average computer running time for each model was about 1.5 h. Figure 2 shows parts of the meshing of the tapered pole with webs (Pole-A). The 3-D element size for the gluelines was 14 mm, which was the maximum executable element size for such thin volumes in ANSYS for this modeling. The element sizes for wood strips and webs were 25 mm and 16 mm, respectively. The meshed volumes shown in the middle of Fig. 2 include a glueline on the top, 4 node-like webs in the middle, and one wood strip on the bottom. The meshing of other gluelines and wood strips is similar to those in the figure and as such is not shown. The top section and the cross-section at the clamped line are highlighted in square frames to give a clear demonstration of the meshing.

A typical predicted deflection curve is shown in Fig. 3, which is a deflection curve of Pole-A that was loaded 667 N at its free end. The experimental deflection values along the pole subjected to the same bending conditions as in the model are also given in the figure. The predicted
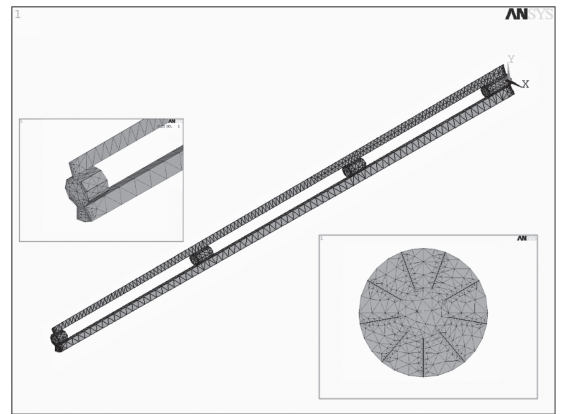

FIG. 2. The meshing of gluelines, wood strips, and node-like webs in the modeling of Pole-A.
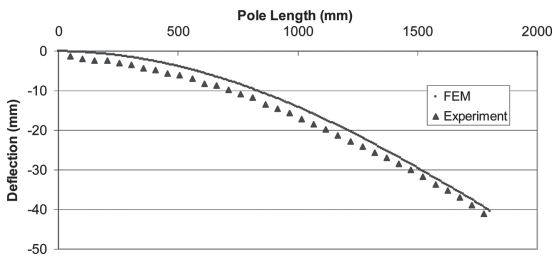
FIG. 3.   Comparison between the deflection predicted by a finite element model and deflection measured in an experiment of a tapered composite pole with plywood node-like webs. The pole was subjected to a 667N concentrated load at its free end.
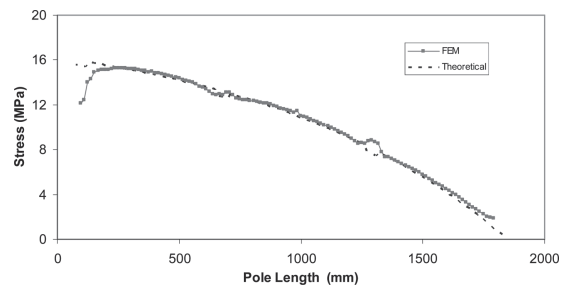

FIG. 4.   FEM-predicted bending stress of a tapered nodal composite pole subjected to a concentrated load at its free end. A calculated bending stress line (dashed) is shown as comparison with the FEM results.

deflection generally agreed with that of the measured data. Similar agreement between the predicted and measured deflection curves was found in the modeling of other tapered and uniform composite poles at all loading levels. All models gave a relatively poor prediction to the measured deflection starting from the clamped line to the middle of the pole length as shown in Fig. 3. Measurement errors in the experiment, averaged constitutive properties used in the modeling, and the limitation of the finite element modeling are a few of the factors that were believed to cause this discrepancy. However, the predicted deflection at the pole free end was close to the measured one for both tapered and uniform composite poles. Similar results were found in our previous study on the finite element modeling of full- and reduced-size composite poles with a uniform diameter through pole length (Piao et al. 2005).

The effects of webs and taper on normal and shear stresses were of the most interest in this study. The installation of the node-like webs increased the moment restraint capability and material thickness of the local cross-sections. The normal and shear stress capacities of these sections were improved by the webs according to Eqs. (1) and (2). Figure 4 shows the normal stress distribution along Pole-A (tapered with webs). As expected, the tension and compression stresses increased from the top to the clamped line of the pole. Stress fluctuation was observed in the web sections and stress concentration was found in the third web from the clamped line.

Figure. 5 shows the normal stress distribution of Pole-B (tapered hollow without webs). The stress variations in the web sections found in Fig. 4 were not present in Fig. 5, indicating that the webs caused the variations of the stress. In order to investigate the stress distribution inside the member, the pole was cut in the YZ plane and in the XY plane at the web and hollow sections. Figure 6 shows the results. The cross-sections in the XY plane at different locations along the pole are shown above the YZ cross-section in the figure. The No. 5 cross-cut in the XY plane gives the stress distribution in the third web. In the enlarged web cross-cut section in the YZ plane shown under web No. 3, a darker stress line at the top edge can be barely identified. Figure 7 shows the stress distribution in XY cross-sections in the No. 3 node and adjacent locations. Stress concentration in the node section was not found in these figures. This indicates that the stress concentration found in Fig.
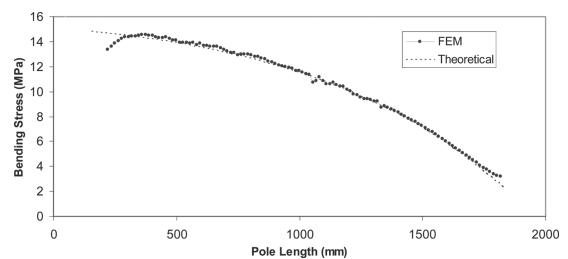

FIG. 5.   FEM-predicted bending stress of a tapered hollow composite pole subjected to a concentrated load at its free end. A calculated bending stress line (dashed) is also given.
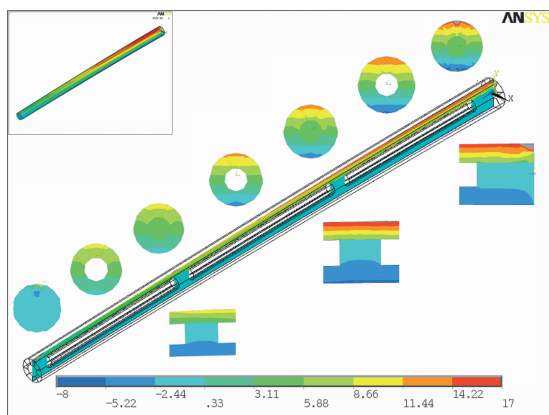
FIG. 6.   Normal stress distribution in the cross-section of Pole-A.

4 likely occurred only on the surface. It is also noted that the node-like webs had little effect on the stress contour in the YZ plane along the pole and in XY plane cross the pole length direction. These figures suggest that the webs had a minor effect on the normal stress along the pole.

The calculated normal stress using Eq. (1) is also shown in Fig. 4 and Fig. 5. The predicted stress distributions for both Pole-A and Pole-B agreed well with those calculated by the theory, except for the sections close to the clamped lines, where the predicted stress by finite element modeling curved down from the maximum toward the clamped lines in both cases, whereas the calculated maximum stress was in the clamped lines. However, in the bending of tapered poles, the failure normally does not occur at the clamped line. The experimental results in our previous study showed that none of the poles totally failed at the clamped line (Piao et al. 2006). Table 3 lists the predicted and experimental maximum stress locations of the five composite poles. In the test of the five poles, Pole-A was the only member that the extreme fiber failure (fiber breakage in the cross fiber direction) started at the clamped line. The failure surface then developed into long shear breakage along the wood grain. Pole-C, Pole-D, and Pole-E all failed at a distance from the clamped lines. The poor prediction of the failure locations by the models shown in Table 3 might be due to the characteristics of the composite poles such as

wood grain directions, property difference among the wood strips, and perhaps different species of southern pine wood.

Figures 8, 9, and 10 show the shear stress on one side of the neutral plane of Pole-A, Pole-B, and Pole-D (uniform diameter with node-like webs), respectively. The dashed lines in Figs. 8 and 9 denote the shear stress calculated using Eq. (2). As expected, the shear stress of the tapered poles (Pole-A, Pole-B, and Pole-C) increased from the clamped lines to the free ends, and the shear stress of the uniform-diameter poles (Pole-D and Pole-E) was uniform throughout the pole length. This indicates that the tip of a tapered pole was one of the weakest sections that are likely subjected to shear failure. The larger the taper angle, the greater the shear will be in the top section. More investigation will be conducted in the next study about the taper effects on shear. Other factors such as shell thickness and gluelines may also affect the shear level. It is expected that greater shell thickness leads to higher shear capacity of the pole. The introduction of node-like webs in the hollow pole is equivalent to increasing the shell thickness. Therefore, the webs at the pole top and along the pole may periodically strengthen the pole against shear. The positive effect of the webs on shear is shown in Fig. 8. When comparing Fig. 8 to Fig. 9, the latter of which shows that the shear stress distribution along Pole-B and the shear stress of Pole-A were reduced in the sections where the webs were installed.

Cross-sections of the members similar to those in normal stress analyses were cut to investigate the shear stress distribution inside the poles. Figure 11 shows the comparison among the shear stress in the XY planes of Pole-A, Pole-B, and Pole-C within the 50-mm-length sections next to the clamped lines. Each column in Fig. 11 has three cross-sections that were cut at the same distance from the clamped lines for Pole-A, Pole-B, and Pole-C (solid tapered composite pole). It is noted that strong shear stress concentration occurred at and close to the clamped lines for all these poles. Stress grades with cone shapes were formed in the bottom of the poles and the central cone showed the high-
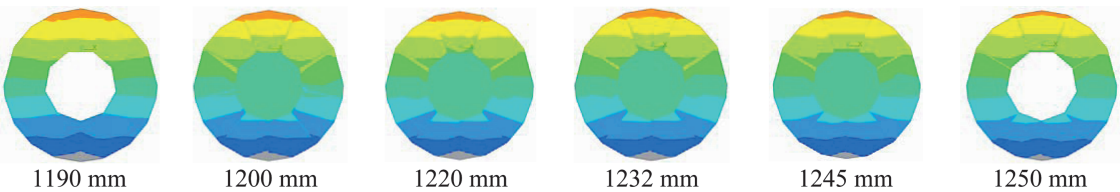
| 1190 mm | 1200 mm | 1220 mm | 1232 mm | 1245 mm | 1250 mm |

FIG. 7.   The normal stress distribution in the XY plane around Web No. III of Pole-A. The locations were measured from the clamped line.

TABLE 3.   *Location of maximum stress of composite poles subjected to 667 N of load at free ends.*

Pole type	Pole-A	Pole-B	Pole-C	Pole-D	Pole-E
Pred. Fail. Loc. (mm)	194	222	128	83	134
Exp. Fail. Loc. (mm)	0	—	50	50	50
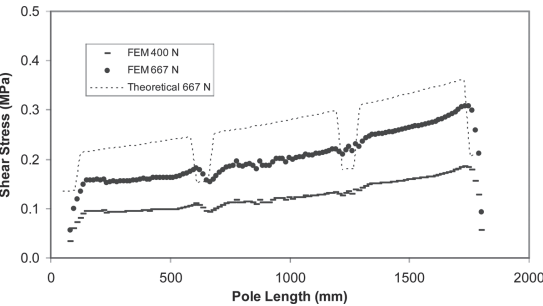
FIG. 8.   FEM-predicted shear stress of a tapered composite pole with node-like webs. The pole was subjected to concentrated loads at its free end.
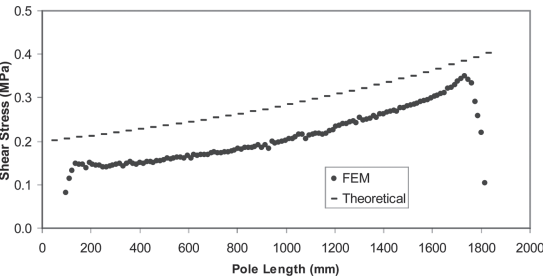

FIG. 9.   Comparison between the FEM-predicted and calculated shear stress of a hollow tapered pole subjected to concentrated loads at its free end.
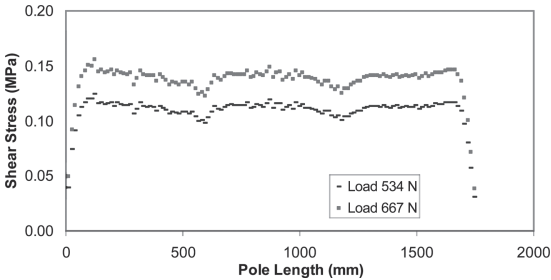

FIG. 10.   FEM-predicted shear stress of the composite pole with uniform diameter and node-like webs. The measured plane was 8.8 mm above the neutral plane.

est shear level, which could be as great as more than 10% of the maximum bending stress under a specific load. Among the three models, the worst case was the hollow pole, Pole-B. Since there is no material in the core to distribute the shear, the pole shell would take all the stress incurred by the vertical load and more stress concentration would occur in the inside surfaces. Compared to Pole-B, the shell of Pole-A should have lower stress levels due to presence of node-like webs in the core. This is evident by comparing the shear distribution in the first and second columns in Fig. 11. In both cases, the node-like webs distributed the shear of the pole.

Figures 12 and 13 show the shear stress distribution in the cross-sections in the YZ and XY planes along Pole-A and Pole-B. The stress distribution inside the webs of Pole-A was detailed below the cross-section in the YZ plane in Fig. 12. Both Figs. 12 and 13 indicated that the shear stress in any cross-section in the XY plane increased from the outside surfaces to the core. The outside surface around the neutral plane had the lowest shear stress, and the inside surface around the neutral plane had the highest. This predicted result could explain why the predicted shear stress was lower than the calculated stress shown in Figs. 8 and 9. It was also observed that in the hollow sections, the shear in the XY plane developed along the gluelines for both cases. This shear development along the gluelines in
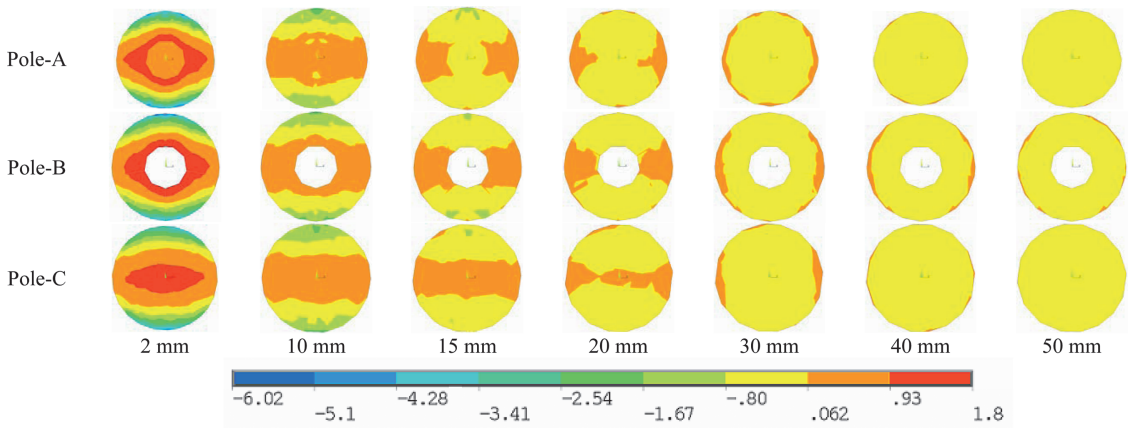
FIG. 11.   Shear stress distribution in the cross-sections of Pole-A and Pole-B. The locations were measured from the clamped ends of the poles.
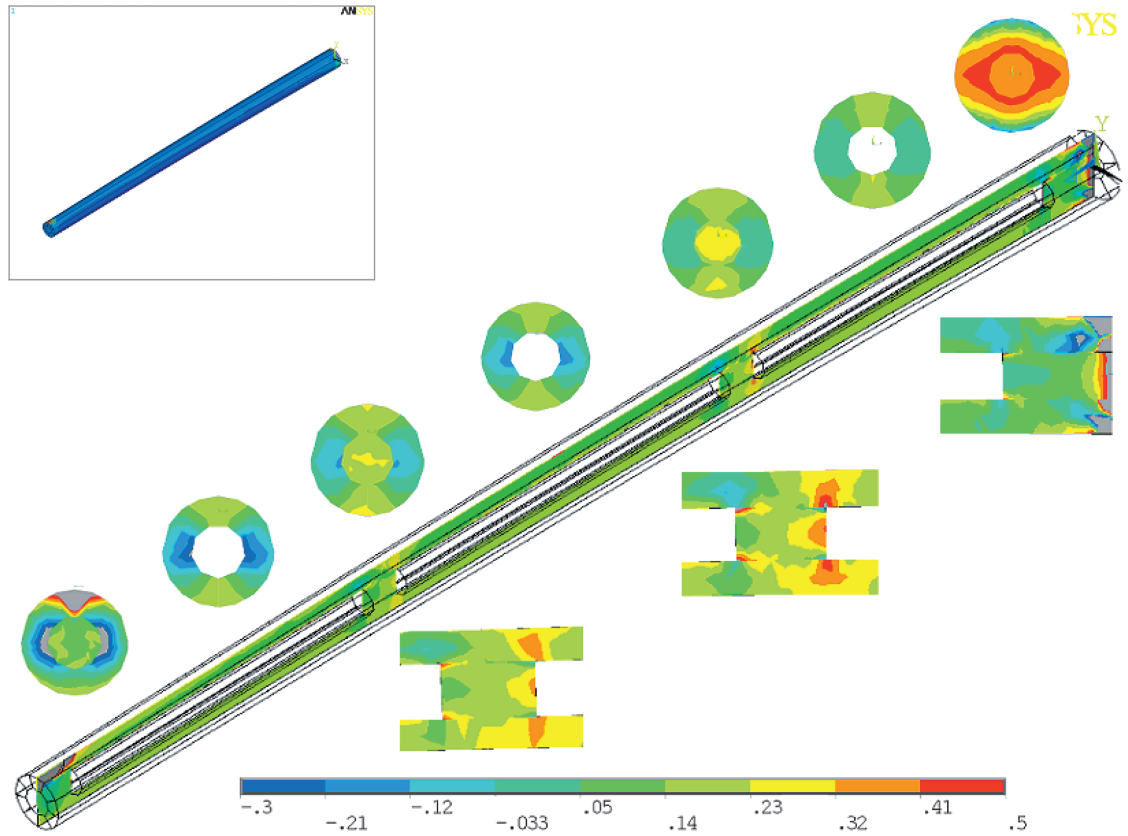

FIG. 12.   Shear stress distribution in the cross-sections of Pole-A subjected to a concentrated load at its free end.

the web sections was found to be less than in the hollow section.

The glueline was another area of interest in this study. As shown in Table 1, the Young's modulus in the *z* direction and shear moduli of the glue were less than those of wood. All these
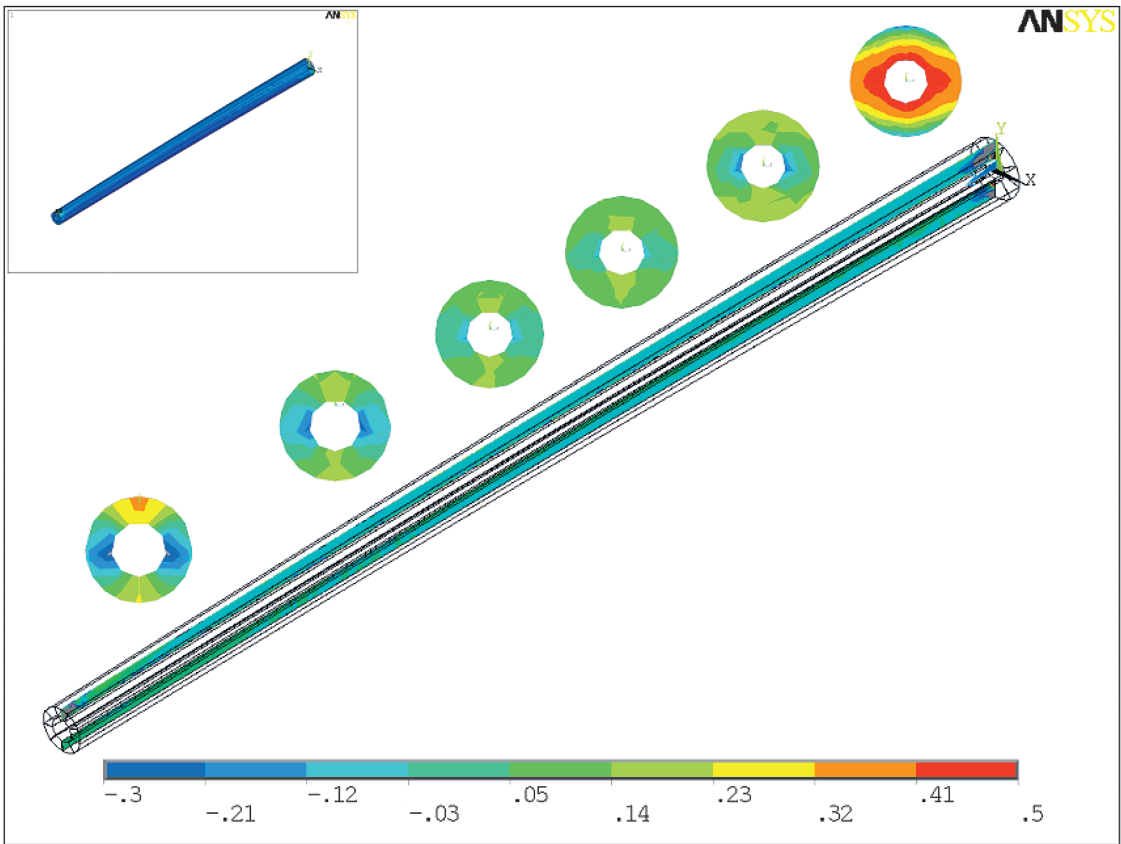
F<small>IG.</small> 13.   Shear stress distribution in the cross-sections of Pole-B subjected to a concentrated load at its free end.

suggested gluelines were the weak sections of the composite poles. Their effects on normal and shear stress distributions can be seen in Figs. 7, 12, and 13. The previous results from the test of Pole-B showed that the pole failed at shear initiated by a bonding defect at the top (Piao et al. 2006). The failure occurred in the gluelines that were subjected to the greatest shear as shown by the No. 6 cross-section in Fig. 13. Processing errors of wood strips, insufficient pressing pressure, and lack of glue in the gluelines may all lead to bonding defects or weak gluelines, which reduced the strength of the poles and should be avoided.

CONCLUSIONS

Five finite element models with ANSYS have been developed and verified with the experiment results. The predicted deflection by these models agreed well with those of the experiment, and the predicted normal stress agreed with those calculated. The normal and shear stress distributions inside the members were investigated, and stress distributions in XY and YZ planes were exhibited. As expected, the node-like webs reduced the local shear stress and improved the shear capacity, especially on the pole top and in clamped line regions where shear levels were the highest, but had little effect on the bending stress. The shear stress increased from the bottom to the top for the members with taper. Large shear stress concentration was predicted in a small region around the clamped lines. The models also predicted that the shear stress of the tapered hollow poles decreased from the inside to the outside surfaces in a cross-section in the

XY plane. Gluelines were the weak regions that were likely subjected to shear failure.

Taper, node-like webs, shell wall thickness, and gluelines were investigated in this study. However, their effects on the performance of composite poles are mostly still unknown and will be investigated in the next study.

REFERENCES

ADAMS, R. D., G. P. KRUEGER, S. LONG, A. E. LUND, AND D. D. NICHOLAS. 1981. Compole™—The composite wood material utility pole. Proc. Am. Wood Protection Assoc. Pp. 1–6.

AMERICAN WOOD PRESERVERS INSTITUTE (AWPI). 1996. Wood Preserving Industry Production Statistical Report. 2750 Prosperity Avenue, Suite 550, Fairfax, VA.

BIOMIMICRY. 2006. http://www.biomimicry.net/intro.html

BRATKOVICH, S. M. 2002. Markets for recycled treated wood products. Pages 37–40 *in* Proc. Enhancing the Durability of Lumber and Engineered Wood Products. Forest Prod. Soc. Madison, WI.

ERICKSON, R. W. 1994. The hollowed veneered pole. Pages 465–468 *in* J. Wells, ed. Proc. Pacific Timber Engineering Conference. Queensland University of Technology, Brisbane, Australia.

———. 1995. Hollow veneered pole. U.S. Patent No. 5,438,812. 1990. Mechanics of materials. 3rd ed. PWS-KENT Publishing Company, Boston, MA. 807 pp.

GERE, J. M., AND S. P. TIMOSHENKO. 1990. Mechanics of materials. 3rd ed. PWS-KENT Publ. Co., Boston, MA. 807 pp.

HOCKADAY, E. 1975. What does structural glue laminated wood have to offer the electrical utility industry. *in* Proc. 6th Wood Pole Institute. Colorado State Univ., Ft. Collins, CO.

MCKAIN, B. 1975. Laminated wood for utilities—A combination of versatility, economics and beauty. Proc. 6th Wood Pole Institute, Colorado State University, Ft. Collins, CO.

MARZOUK, H. M., M. U. HOSEIN, AND V. V. NEIS. 1978. Built-up utility poles using prairie timber. Forest Prod. J. 28(11):49–54.

PIAO, C., T. F. SHUPE, AND C. Y. HSE. 2004. Mechanical properties of small-scale wood-laminated composite poles. Wood Fiber Sci. 36(4):536–546.

———, ———, R. C. TANG, AND C. Y. HSE. 2005. Finite element analyses of wood-laminated composite poles. Wood Fiber Sci. 37(3):535–541.

———, ———, ———, AND ———. 2006. Mechanical properties of small-scale laminated wood composite poles: Effects of taper and webs. Wood Fiber Sci. 38(4):633–643.

SHIDLES, J. B. SC. 1970. Adhesive Handbook. CRC Press, A Division of the Chemical Rubber Co., Cleveland, OH.

TANG, R. C., AND S. F. ADAMS. 1973. Application of reinforced plastics for laminated transmission poles. Forest Prod. J. 23(10):42–46.

USDA FOREST PRODUCTS LABORATORY (USDA FPL). 1999. Wood handbook-Wood as an engineering material. Gen. Tech. Rep. FPL-GTR-113. USDA Forest Service, Forest Prod. Lab., Madison, WI. 463 pp.